Plant Pathol. J. 39(2) : 191-206 (2023)
https://doi.org/10.5423/PPJ.OA.08.2022.0119
eISSN 2093-9280

The Plant Pathology Journal

Research Article **Open Access**

Comparative Genomic Analysis and Rapid Molecular Detection of *Xanthomonas euvesicatoria* Using Unique ATP-Dependent DNA Helicase *recQ*, *hrpB1*, and *hrpB2* Genes Isolated from *Physalis pubescens* in China

Faisal Siddique, Yang Mingxiu, Xu Xiaofeng, Ni Zhe, Haseeb Younis, Peng Lili, and Zhang Junhua *

College of Agriculture, Northeast Agricultural University, Harbin 150030, China

(Received on August 31, 2022; Revised on January 4, 2023; Accepted on March 7, 2023)

Ground cherry (*Physalis pubescens*) is the most prominent species in the *Solanaceae* family due to its nutritional content, and prospective health advantages. It is grown all over the world, but notably in northern China. In 2019 firstly bacterial leaf spot (BLS) disease was identified on *P. pubescens* in China that caused by both BLS pathogens *Xanthomonas euvesicatoria* pv. *euvesicatoria* resulted in substantial monetary losses. Here, we compared whole genome sequences of *X. euvesicatoria* to other *Xanthomonas* species that caused BLS diseases for high similarities and dissimilarities in genomic sequences through average nucleotide identity (ANI) and BLAST comparison. Molecular techniques and phylogenetic trees were adopted to detect *X. euvesicatoria* on *P. pubescens* using *recQ*, *hrpB1*, and *hrpB2* genes for efficient and precise identification. For rapid molecular detection of *X. euvesicatoria*, loop-mediated isothermal amplification, polymerase chain reaction (PCR), and real-time PCR techniques were used. Whole genome comparison results showed that the genome of *X. euvesicatoria* was more closely relative to *X. perforans* than *X. vesicatoria*, and *X. gardneri* with 98%, 84%, and 86% ANI, respectively. All infected leaves of *P. pubescens* found positive amplification, and negative controls did not show amplification. The findings of evolutionary history revealed that isolated strains XeC10RQ, XeH-9RQ, XeA10RQ, and XeB10RQ that originated from China were closely relative and highly homologous to the *X. euvesicatoria*. This research provides information to researchers on genomic variation in BLS pathogens, and further molecular evolution and identification of *X. euvesicatoria* using the unique target *recQ* gene through advance molecular approaches.

Keywords **:** Identification, PCR, *P. pubescens*, *recQ*, *Xanthomonas*

*Corresponding author.
Phone) +86-18646561068, FAX) +86-0451-55190447
E-mail) zhangjunhua@neau.edu.cn, podozjh@163.com
ORCID
Zhang Junhua
https://orcid.org/0000-0002-6899-3278

Handling Editor : Hyun Gi Kong

The ground cherry (*Physalis pubescens*), also known as golden strawberry, Chinese lantern, low ground cherry, hairy ground cherry, and husk tomato, is one of the most well-known species (El Sheikha, 2004; USDA Natural Resources Conservation Service, 2016). It is grown in tropical, subtropical, and temperate climates all over the world, including the United States, Mexico, Colombia, Egypt, Zimbabwe, Kenya, Madagascar, and South Africa, but it is especially popular in Northeast China for the reason of its delicious flavor, nutritional content, and prospective health welfares (Hao et al., 2017). Vitamin C, potassium, phosphorus, zinc, boron, polyphenols, and carotenoids are all found in abundance in *P. pubescens.* It also contains a good amount of important amino acids including valine, tryptophan and isoleucine, which is necessary for the health of human being (El Sheikha et al., 2010).

However, occurrence of bacterial leaf spot (BLS) disease on *P. pubescens* caused significant economic losses (Song et al., 2019). *Xanthomonas euvesicatoria*, *X. vesicatoria*, *X. gardneri*, and *X. perforans* are four the genospecies of *Xanthomonas* that have been associated to BLS disease (Jones

et al., 2004; Kebede et al., 2014). It is a gram-negative rod-shaped bacterium using aerobic motility and a single polar flagellum. The host range of BLS included *Solanum lycopersicum* var. *cerasiforme*, *Lycopersicon pimpinellifolium*, *S. lycopersicum*, *Capsicum annuum*, *C. anomalum*, *C. frutescens*, *C. baccatum*, and *C. chinensis* (Baker et al., 2014; EFSA Panel on Plat Health, 2014).

Nevertheless, according to Song et al. (2019), *P. pubescens* was new host range in BLS caused by *Xanthomonas euvesicatoria* pv. *euvesicatoria* that affected the quality and quantity of the fruit. Furthermore, the leaf becomes circular water soaked lesions on the lower and upper epidermis in the early stages of infection, and the leaf spot gradually rises and then turns from white to dark brown until it reaches the necrotic stage with a chlorotic edges. Occasionally, leaf spots are covered with a black color and greasy appearance, and bacterial populations grow on nutrient agar resulting in yellow colonies, indicating the presence of *Xanthomonas* species (Song et al., 2019).

Comparative genomics is essential for obtaining information from biological sequences. Comparative genomics of pathogenic bacteria has helped to find out genetic determinants of pathogenicity and virulence, as well as provide insights into pathoadaptation evolution (Garita-Cambronero et al., 2018). Larrea-Sarmiento et al. (2018) performed 10 genomic comparative analysis of BLS pathogens (*X. euvesicatoria*, *X. perforans*, *X. vesicatoria*, and *X. gardneri*) with other BLS pathogens for genomic variation and target gene selection through average nucleotide identity (ANI) and BLAST comparison.

Gene selection is critical pneumonia for accurate evolution and identification of BLS pathogens. Accordingly, *hrpB1* and *hrpB2* colocalize in the periplasm and interact with hrcD, implying that they are part of the type 3-secretion system's (T3SS) periplasmic substructure. *X. euvesicatoria* delivers effector proteins into host cells through the T3SS to stimulate disease and T3SS transforms an active catalytic serine/threonine protein kinase in plant cells, resulting in novel enzymatic activity. The T3SS, which releases effector proteins into host cells to weaken plant immunity and promote disease, is essential for *Xanthomonas* pathogenicity (Teper et al., 2016). The T3SS was necessary for reliable identification of the BLS pathogens (Larrea-Sarmiento et al., 2018). ATP-dependent DNA helicases RecQ is genome surveillance proteins that can be found throughout the animal kingdom. RecQ helicases are bacterial, fungal, animal, and plant genome surveillance proteins. RecQ family members are involved in gene targeting, DNA repair, and development (Mendonca et al., 1995). The identification of DNA repair genes in phytopathogens could aid in the understanding of the methods by which these organisms adapt to their surroundings, including plant infection (Martins-Pinheiro et al., 2004).

Further research into evaluating and detecting pathogens at the molecular level requires the selection of approaches that allow for easy and rapid detection. Since the 1990s, more laboratories have begun to use polymerase chain reaction (PCR) and its derivatives, such as digital PCR, multiplex PCR, nested-PCR, and quantitative PCR (qPCR), for pathogen recognition and identification of *Xanthomonas* species (Strayer et al., 2016; Yasuhara-Bell et al., 2017; Zhang and Tanner, 2017). Such approaches are typically highly specific, comparatively fast, and inexpensive, but they do have certain drawbacks, such as the need for specific equipment and skilled workers in most circumstances. New technologies based on isothermal amplification of DNA, such as, helicase-dependent amplification, recombinase polymerase amplification, and loop-mediated isothermal amplification (LAMP) have emerged in the first few years of this century, ability to overcome some of the disadvantages of PCR-based approaches (Larrea-Sarmiento et al., 2018; Zhong and Zhao, 2018).

In comparison to other molecular approaches, the LAMP method allows for the easy and rapid detection of pathogens in a short period. LAMP is a DNA polymerase with two interior primers, and two exterior primers, and the interior primer binds to its F2c or B2c primer on the objective DNA, while the exterior primer binds to its F3c or B3c primer, creating a single complementary sequence. At both ends of a DNA sequence, internal loop primers (LF and LB) have the ability to speed up and shorten the reaction time (Larrea-Sarmiento et al., 2018). Moreover, identification and pathogenicity characterization of *Xanthomonas euvesicatoria* pv. *euvesicatoria* reported on *P. pubescens* in China by concatenated phylogeny based on hrpB and four housekeeping genes (*lepA-gyrB-gapA-gltA*) (Song et al., 2019). Despite the occurrence of BLS outbreaks on *P. pubescens* in China, little study has been undertaken on the genetic characterization and distribution of the pathogenic *Xanthomonas* species on *P. pubescens*. The major goal of this study was to isolation and characterization of BLS strains isolated from *P. pubescens* in China and to develop genome wide comparison of 13 *Xanthomonas* spp. using NCBI whole genome sequence database to verify genomic diversification and showed site location of selected three genes (T3SS *hrpB1* and *hrpB2* genes and ATP-dependent DNA helicase *recQ* gene). Furthermore, to develop molecular detection methods from unique genomic sequences, identified by comparative genomics, which can distinguish different *Xanthomonas* pathotypes infecting *P. pubescens*.

In addition, an evolutionary study was performed to ascertain the strains' phylogenetic position within the *Xanthomonas* species.

Materials and Methods

Sample collection, isolation, and DNA extraction. Infected 52 specimens were taken from different areas of Heilongjiang Province, China, based on symptoms (circular water-soaked lesions, leaf spot with dark brown spot, and necrotic stage with chlorotic margin). The infected samples were cut into small pieces, dipped in 2% sodium hypochlorite, and then transferred to phosphate buffered saline for one day. They were then made into a suspension of 1×10^5 solution for the isolation of the bacterial strains cultured on nutrient agar in the Petri plate and incubated at 28°C for three days. A single colony was chosen and streaked numerous times on nutrient agar for pure culture. DNA was extracted from diseased and healthy plant material using the CTAB technique. This extracted DNA was kept at −80°C for subsequent analysis.

Whole genome sequence comparison, target selection, and gene location. Whole genome sequence data of 13 *Xanthomonas* strains were retrieved from NCBI GenBank database. The investigation of whole genome sequence comparison was carried out using binary methods: BLAST comparison and ANI. CGview Server assessed the blast comparison, while OrthoANI software (OAT) Lee et al. (2015) analyzed the ANI for more similarities and differences among the genomes. In whole genomes sequence analysis, *X. euvesicatoria* was compared with *X. perforans*, *X. vesicatoria*, *X. gardneri*, *X. axonopodis* pv. *citrumelo*, *X. compestris* pv. *vesicatoria*, *X. arboricola* pv. *pruni*, *X. cucurbitae*, and *X. fragariae* that casual agents of bacterial spot and other *X. campestris* pv. *campestri*, *X. axonopodis* pv. *glycines*, *Xanthomonas translucens* pv. *translucens*, and *X. vasicola* caused black rot, bacterial pustules and bacterial leaf streak diseases, respectively. Genomes of *X. euvesicatoria* (CP018467), *X. axonopodis* pv. *citrumelo* (CP002914), *X. gardneri* (CP018731), *X. perforans* (CP019725), *X. campestris* pv. *vesicatoria* (CP017190), and *X. campestris* pv. *vesicatoria* (AM039952) were aligned with progressive MAUVE for more compatibility among genomes and exact gene location of *recQ* gene in all genomes. CGview Server was also used to find the exclusive location of the ATP-dependent DNA helicase *recQ* gene in the *X. euvesicatoria*, which was used to construct specialized LAMP primers for the *X. euvesicatoria*.

Primer design, PCR protocol, and sequencing. Plant pathogen bacteria can be detected using PCR, which is a relatively easy and convenient approach. Three genes (*hrpB1*, *hrpB2*, and *recQ*) were chosen in this investigation for accurate identification of pathogenic strains *X. euvesicatoria* through PCR analysis. *hrpB1* and *hrpB2* primers were designed through Primer3 software, whereas *recQ* primer was designed by Primer Explorer V5 and additionally, F3 as a forward and B3 as a reverse primer used for PCR analysis (Table 1). Each PCR tube had a total of 25 µl of reaction, which contains 2 µl of template DNA and 0.4 µM, 0.4 µM, and 12.5 µl of forward primer, reverse primer, and 2× Taq Master Mix, respectively (CoWin Biosciences, Beijing, China) and remaining volume cover with dd water. The cycling conditions were 3 min at 94°C, 35 cycles of denaturation at 94°C for 30 s, and annealing at 54°C for 30 s for both genes *hrpB1* and *hrpB2* whereas for *recQ* was at 53°C for 30 s, elongation at 72°C for 30 s, and a final elongation at 72°C for 10 min. PCR products were run on 1% agarose gel electrophoresis with 200 mA for 25 min. and then, PCR products sent to Sangon Biotech (Shanghai) Co., Ltd. (Shanghai, China) for sequencing.

Primer design for LAMP. To create specific LAMP primers for *X. euvesicatoria*, the ATP-dependent DNA helicase *recQ* gene was chosen. The specificity of this gene is important for genomic stability. Primer Explorer V5 software (https://primerexplorer.jp/e/) was used to construct sense and anti-sense primers of inner (FIP and BIP), outer (F3 and B3), and internal loop primers (LF and LB) (Table 1). Each primer was verified in silico using the BLASTn tool in the NCBI nucleotide database. The designed primers covered 100% of the query and were 100% identical to *X. euvesicatoria.*

Optimization of LAMP reaction. The evaluation of LAMP chemicals reaction was performed by optimization of reaction with different concentrations such as DNA template concentrations (10^{-1}, 10^{-2}, 10^{-3}, 10^{-4}, and 10^{-5}), primers (1:2, 1:4, 1:8, and 1:12), $MgSO_4$ (0, 4, 5, 6, 7, and 8 mM), time (15, 30, 45, and 60 min), temperature (57°C, 59°C, 61°C, 63°C, 65°C, 67°C, and 69°C), Bst (0.5, 1, 1.5, and 2), betaine (0.4, 0.6, 0.8, 1, 1.2, and 1.4 M), and hydroxynaphthol blue (HNB) for visual color change.

The final reaction mixture of 25 µl contains 2 µl of template DNA, primer (F3 and B3 as outer primer, FIP and BIP as inner primers), $MgSO_4$, 1.4 mM of dNTPs, 1× isothermal amplification buffer (containing 20 mM Tris-HCl, 10 mM $(NH_4)_2SO_4$, 50 mM KCl, 2 mM $MgSO_4$, and 1% Tween 20 with pH 8.8), 1 U of Bst 2.0 WarmStart DNA

Table 1. List of primers used in this study

Primer name	Primer sequence (5′-3′)	Length (bp)	Target gene	GC (%)	Tm (°C)	Amplicon size (bp)	Detection method	Reference
RQX-F3	5′-GACCCAGCTGTTTGATACGT-3′	20	recQ	50	59.5	175	LAMP, PCR, RT-PCR	This study
RQX-B3	5′-GCTTCGGCGAGACCTATG-3′	18	recQ	61	59			
RQX- FIP	5′-TGTATCGCAGCGGGCAGC-GC-TACCGCGCAGGATG-3′	34	recQ	67, 69	64, 59		LAMP	This study
RQX- BIP	5′-GCCTTCTGCGAGGCTACCC-CCAAACCCTGCGGCAAT-3′	36	recQ	68, 59	64, 59			
RQX-LF	5′-GGCGTGGGCCATCTGAT-3′	17	recQ	65	61		LAMP	This study
RQX- LB	5′-CGGGGTCAGGCAGTTGT-3′	17	recQ	65	60			
HB1-F	5′-CACCTTCCACGTAATTGCCG-3′	20	hrpB1	55	59	160	PCR	This study
HB1-R	5′-AGTGGGCTCATCGAACTGA-3′	19	hrpB1	52	58			
HB2-F	5′-GGTGGTCGATGTGCAGAAC-3′	19	hrpB2	57	58	155	PCR	This study
HB2-R	5′-TGACATTGAGGTTGAAGCCG-3′	20	hrpB2	50	58			

LAMP, loop-mediated isothermal amplification; PCR, polymerase chain reaction; RT-PCR, reverse transcription polymerase chain reaction.

polymerase, betaine, and sterile double-distilled water. The experiment was carried out in a thermal water bath for the time between 15 to 60 min at a temperature between 57°C to 69°C. To confirm amplification, the amplified LAMP products 4 µl were examined on a 2% stained agarose gel with ethidium bromide.

Real-time PCR assay. The SYBR Green real-time PCR assay was used to test the infected samples of *P. pubescens* using target RecQ gene. iTaq Universal SYBR Green Supermix kit (Bio-Rad, Hercules, CA, USA) used for real-time PCR that contains dNTPs, iTaq DNA Polymerase, $MgCl_2$, SYBR Green I, enhancers, stabilizers, and a blend of passive reference dyes. Each PCR reaction tube contained 10 µl of iTaq Universal SYBR Green Supermix kit and 0.4 µl of each 10 µmol/l primer, 1 µl template, and 8.6 µl ddH_2O. Real-time PCR was performed with the following program: 2 min at 95°C, 30 cycles of denaturation at 95°C for 15 s, annealing at 54°C for 15 s, elongation at 72°C for 15 s, and a final elongation at 72°C for 2 min. DNA templates were replaced by double-distilled water as a negative control.

Phylogenetic tree analysis and model design. Phylogenetic trees were constructed using three unique target genes *hrpB1*, *hrpB2*, and *recQ*. PCR products were purified and sequenced by Sangon Biotech (Shanghai) Co., Ltd. All other sequenced data were retrieved from NCBI GenBank database and a basic alignment search technique (BLASTn) was used to match the unidentified sequences to sequences in public databases. All sequenced data were aligned through ClustalW integrated into MEGA 11 software. Evolutionary tree analysis was performed through maximum likelihood (ML) methods. In the evolutionary tree-building process, model selection is a critical phase. To estimate phylogeny, we employed standard DNA sequence evolution models. MAGA 11 was used to build 24 nucleotide substitution fit models.

Pathogenicity and specificity test of primers for *recQ*, *hrpB1*, and *hrpB2* genes. On five cultivars of *P. pubescens*, bacterial isolates were tested for pathogenicity, and inoculation was done on seedlings that were five to six weeks old. The reference strains (Xeu1, Xeu2, and Xeu3) were cultured on nutritional agar (NA) medium in a Petri dish for three days at 28°C. Bacterial suspensions having 1×10^5 cfu/ml were prepared through 10-fold dilutions into nutrient broth medium, and spectrophotometrically adjusted suspensions 0.03 at 600 nm OD for inoculation.

Through needleless syringes, suspensions were injected into the anterior portion of the mesophyll of immature leaves and for control treatment, healthy leaf was used. Plants were placed into growth chamber with a photoperiod of 12 h and 28 ± 1°C and leaves were observed on daily bases. Re-isolation of infected leaves and growth on NA described above and in addition, extraction of DNA of infected leaves and non-template control (NTC) through CTAB method and performed PCR using primers of *hrpB1*, *hrpB2*, and *recQ* genes.

Furthermore, for the primer specification of *hrpB1*, *hrpB2*, and *recQ*, 52 strains were used including three reference strains (Xeu1, Xeu2, and Xeu3), two strains of

Pseudomonas syringae pv. *syringae* (Pss1 and Pss2) and one strain of *X. oryzae* pv. *oryzae* (YH). These strains were collected from Plant Pathology Lab of Northeast Agricultural University and DNA was extracted through CTAB method. All these strains were observed through conventional PCR approach and after that run on 1% agarose electrophoresis gel with 200 mA for 25 min. Three strains, Xeu1, Xeu2, and Xeu3, were obtained from Song et al. (2019) for validation of *X. euvesicatoria* with *recQ*, *hrpB1*, and *hrpB2* genes and these strains were applied to *P. pubescens* seedlings using the inoculation procedures described above.

The Canopeo app (https://canopeoapp.com) was used to calculate the leaf damage area by percentage at 3, 7, 14, and 21 days after inoculation to determine disease severity. Canopeo is a system-consuming RGB (red, green, and blue) programmer. The excess ratios of the B/G, R/G and green indexes were employed to construct pixel analysis. The results are represented in binary pictures, with white pixels indicating that the selection criteria were met (green canopy), and black pixels indicating that the selection criteria were not met (not green canopy) or that damage occurred (Patrignani and Ochsner, 2015). The percentage of leaves that have green color was used to determine severity; a score of 100% was connected with non-infected or healthy leaves, *Xanthomonas* infected leaves were associated with decreased percentages.

Results

Whole genome sequence comparison and selection of target gene. For more similarities or differences throughout 13 genomes, CGview Server was used to do whole genome sequence comparison analysis. The sequence data for whole genomes comparison was obtained from the NCBI GenBank genome. BLAST comparison and ANI are two extensively used methods for genomic comparison. Genome of *X. euvesicatoria* compared with other 12 genomes with the location of specific target gene *recQ* ATP-dependent DNA helicase and *hrpB* (*hrpB1* and *hrpB2*) (Fig. 1). When compared to other genomes, the sequence of the reference genome *X. euvesicatoria* was closely related to the sequences of *X. campestris pv. vesicatoria* 85-10, *X. axonopodis pv. citrumelo* F1, and *X. perforans* LH3.

ANI calculation is one of the main aspects and approaches for comparative genomic data and taxonomic purposes. Furthermore, using OAT (Lee et al., 2015), ANI analysis revealed that pairwise identity between *X. euvesicatoria*

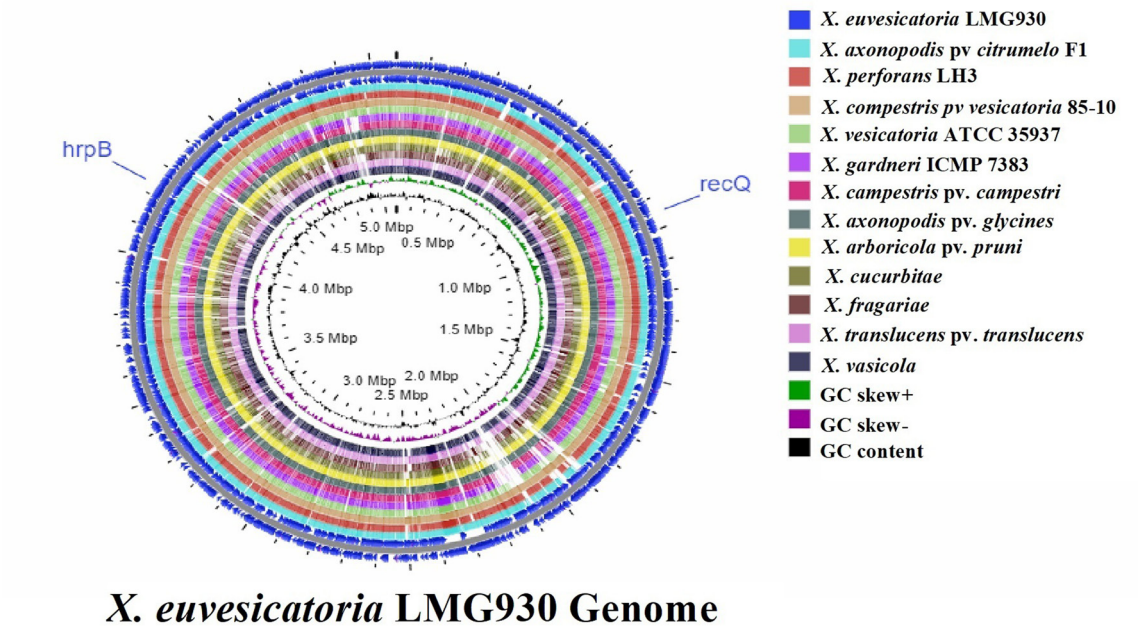

Fig. 1. Target gene selection and genomic variation among 13 whole genomes. Circular whole genome comparison was performed by CGview Server that showed location of *recQ* and *hrpB* genes with GC content and GC skew (positive and negative). In this image *Xanthomonas euvesicatoria* strain LMG930 compared with *X. perforans*, *X. vesicatoria*, *X. gardneri*, *X. axonopodis* pv. *citrumelo*, *X. compestris* pv. *vesicatoria*, *X. arboricola* pv. *pruni*, *Xanthomonas cucurbitae*, and *X. fragariae* that casual agents of Bacterial spot and other *X. campestris* pv. *campestri*, *X. axonopodis* pv. *glycines*, *Xanthomonas translucens* pv. *translucens*, and *X. vasicola* cause black rot, bacterial pustules, and bacterial leaf streak diseases, respectively.

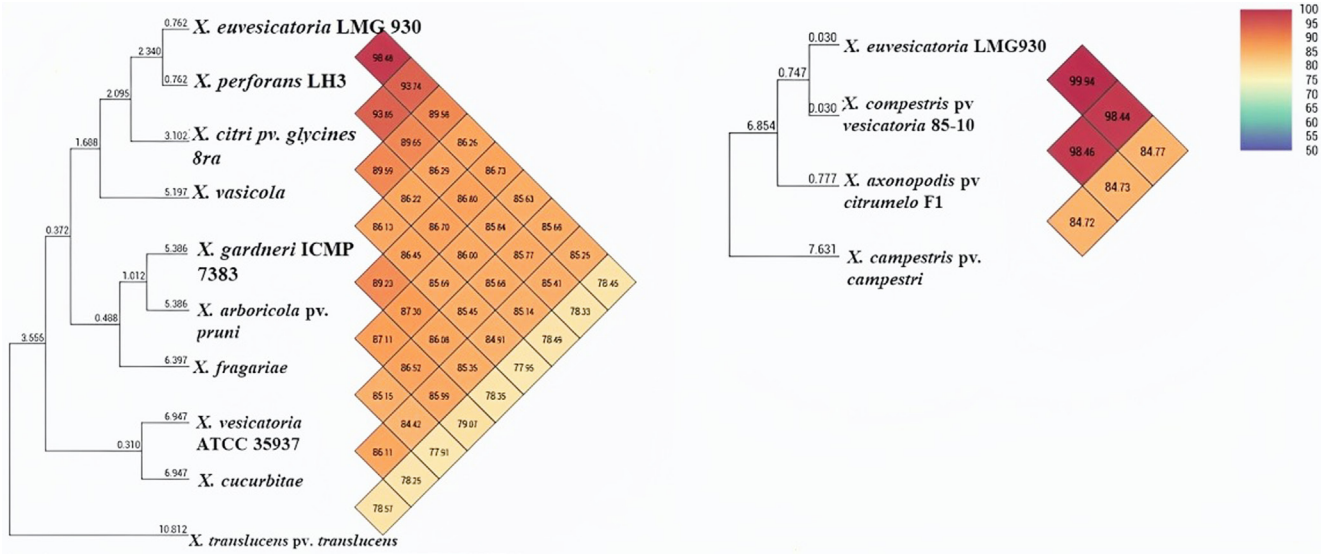

Fig. 2. Phylogenetic tree show average nucleotide identity of all genome involved in circular genome comparison. *Xanthomonas euvesicatoria*, *X. perforans*, *X. axonopodis* pv. *citrumelo*, and *X. compestris* pv. *vesicatoria* were closely relative to each other and clusterd in one group while *X. vesicatoria* and *X. gardneri* were existed in another group that cause bacterial leaf spot disease.

and *X. compestris* pv. *vesicatoria* was 99.9%, indicating high similarity among the genomes, while *X. axonopodis* pv. *citrumelo* and *X. perforans* showed 98.48% and 98.46% similarity, respectively (Fig. 2). *X. gardneri* and *X. vesicatoria* found 86% ANI homology that was less similar as compared to other BS-causing *Xanthomonas* species. Additionally, *X. euvesicatoria* and *X. compestris* pv. *vesicatoria*, *X. perforans*, and *X. axonopodis* pv. *citrumelo* were clustered in one group and showed 99% to 98% homology, but *X. gardneri* and *X. vesicatoria* were recognized in another group and showed less homology.

Gene selection was aided by mauve-based progressive multiple genome sequence alignments. Genomes of *X. campestris* pv. *vesicatoria* (CP017190), *X. perforans* (CP019725), *X. euvesicatoria* (CP018467), *X. axonopodis* pv. *citrumelo* F1 (CP002914), *X. gardneri* (CP018731), and *X. campestris* pv. *vesicatoria* (AM039952) were aligned through progressive mauve software. Progressive mauve generates multiple genome alignments, which can be used for comparative genomic and population genomic investigations. In this study, multiple alignments of six genomes were used for the identification and location of ATP-dependent DNA helicase *recQ* gene (Supplemenary Fig. 1). In multiple alignments, each genome is laid out horizontally, with homologous portions indicated as colored rectangles in locally collinear blocks (LCBs). Syntenic regions showed by boxes of the same color, inverted regions engaged by boxes below the horizontal strain line, and rearrangement indicated by colored lines (Supplementary Fig. 1).

Multiple alignments showed that *X. euvesicatoria* and *X. perforans* were closely relative at regions inverted with homologous segments LCBs. On the other hand, *X. axonopodis* pv. *citrumelo* (CP002914), *X. campestris* pv. *vesicatoria* (CP017190) and *X. campestris* pv. *vesicatoria* (AM039952) were closely relative at syntenic regions. In contrast, *X. gardneri* (CP018731), was not much closer to *X. euvesicatoria* and *X. perforans*, some region was at inverted and some in the syntenic region. Lines collate aligned segments between genomes.

The gene encoding ATP-dependent DNA helicase *recQ* was located at position 3516837-3518633 bp in the genomes of *X. euvesicatoria* (CP018467), *X. axonopodis* pv. *citrumelo* F1 (CP002914), *X. gardneri* (CP018731), *X. perforans* (CP019725), *X. campestris* pv. *vesicatoria* (CP017190), and *X. campestris* pv. *vesicatoria* (AM039952) (Supplementary Fig. 1). Interestingly, the genes located upstream and downstream were highly similar in the six genomes. *recQ* gene was exploited as a target gene to identify *X. euvesicatoria* on the *P. pubescens* host and design primers for molecular techniques such as LAMP, PCR, and reverse transcription polymerase chain reaction (RT-PCR).

Homologous gene analysis of target genes *recQ*, *hrpB1*, and *hrpB2*. Comparative analysis of 13 genomes were

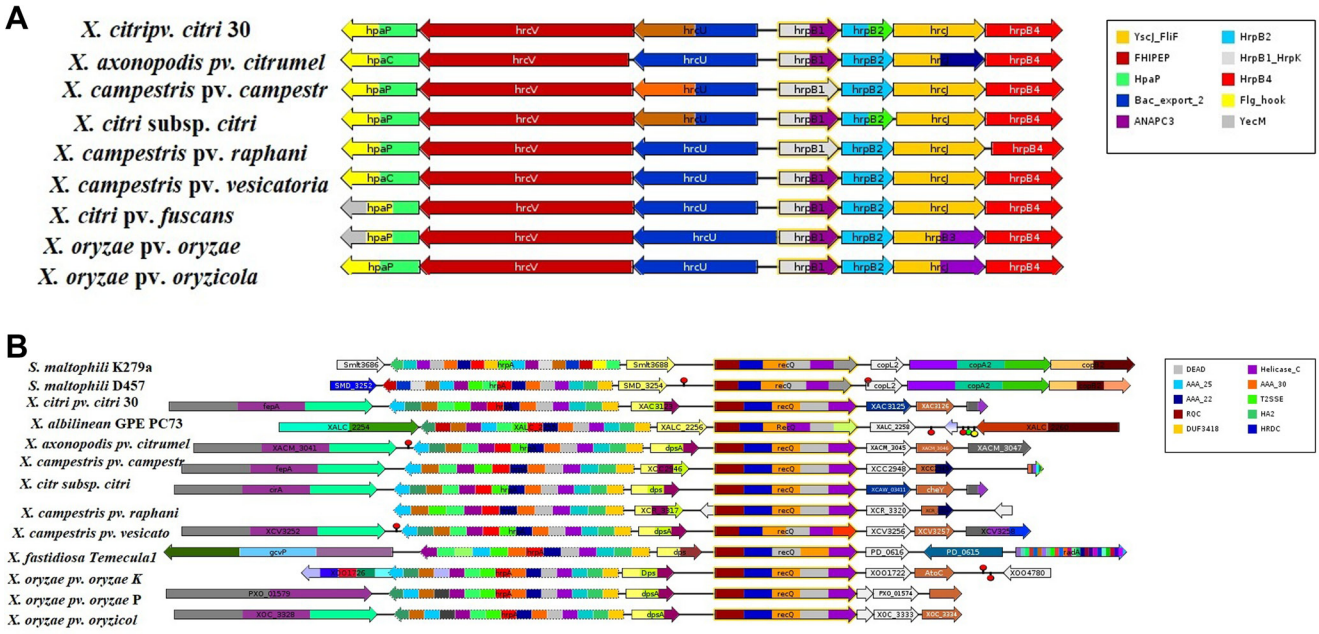

Fig. 3. (A, B) Schematic diagram of different *Xanthomonas* spp. that belong to *Xanthomonadales* order such as *Stenotrophomonas maltophilia* K279a, *Stenotrophomonas maltophilia* D457, *Xanthomonas citri* pv. *citri* 306, *Xanthomonas albilineans* GPE PC73, *Xanthomonas axonopodis* pv. *citrumelo* F1, *Xanthomonas campestris* pv. *campestris* ATCC 33913, *Xanthomonas citri* subsp. *citri* Aw12879, *Xanthomonas campestris* pv. *raphanin* 756C, *Xanthomonas campestris* pv. *vesicatoria* 85-10, *Xylella fastidiosa* Temecula1, *Xanthomonas oryzae* pv. *oryzae* KACC 10331, *Xanthomonas oryzae* pv. *oryzae* PXO99A, *Xanthomonas oryzae* pv. *oryzicola* BLS256 for homologous analysis of *hrpB1*, *hrpB2*, and *recQ* genes. This figure showed that different genes existing of *Xanthomonas* spp. with short conserved sequence pattern associated with distinct functions of a protein. It also showed neighborhood's genes to *hrpB1*, *hrpB2*, and *recQ* genes.

also performed through GeConT (Ciria et al., 2004) using BLAST modules for specific genes localization and homologous gene analysis in the selected genomes. In this study, results showed that all the genomes showed *recQ* gene with different motifs in Figure. *recQ* gene motifs showed on the different protein families such as RecQ Zn binding, RQC domain, HRDC domain, DEAD/DEAH box helicase, helicase conserved C-terminal domain and protein of unknown function (DUF2385). Furthermore, *recQ* gene existing in superfamily II DNA helicase on the cluster of orthologous groups. *recQ* gene of *X. campestris* pv. *vesicatoria* 85-10 neighborhood to *dpsA* gene that is DNA-binding related protein (Fig. 3B). On the other hand, visualizing the genome context of the *hrpB1* and *hrpB2* genes was also analyzed. In all genomes, *hrpB1* was shown on HrpB1_HrpK motif which indicated the bacterial type III secretion protein while *hrpB2* showed on HrpB2 motif which also indicated the bacterial type III secretion protein. *hrpB1* and *hrpB2* genes also showed neighborhood genes (Fig. 3A).

PCR assay and confirmation of primers. All designed primers were tested by Blastn in the NCBI GenBank database for confirmation of *Xanthomonas* spp., which revealed 100% query and identity with *Xanthomonas* species that cause BLS disease. Infected samples taken from the field were subjected to conventional PCR with *hrpB1, hrpB2*, and *recQ* genes. All of the infected samples showed positive amplification with amplicon size 160 bp, 155 bp, and 175 bp on 1% agarose gel electrophoresis using *hrpB1*, *hrpB2*, and *recQ* genes, respectively (Fig. 4). Therefore, positive amplification detected infected samples, whereas positive amplification was not observed in the negative control or healthy leaf samples. Furthermore, sequencing products were sent to Sangon Biotech (Shanghai) Co., Ltd. of three selective genes for molecular characterization and further analysis.

Efficiency of the LAMP assay. We used the LAMP assay with a variety of LAMP reagent doses, intervals, and temperatures to find the best reaction system for detecting *X. euvesicatoria* using the *recQ* ATP-dependent DNA helicase gene. Results indicate that the best concentrations of

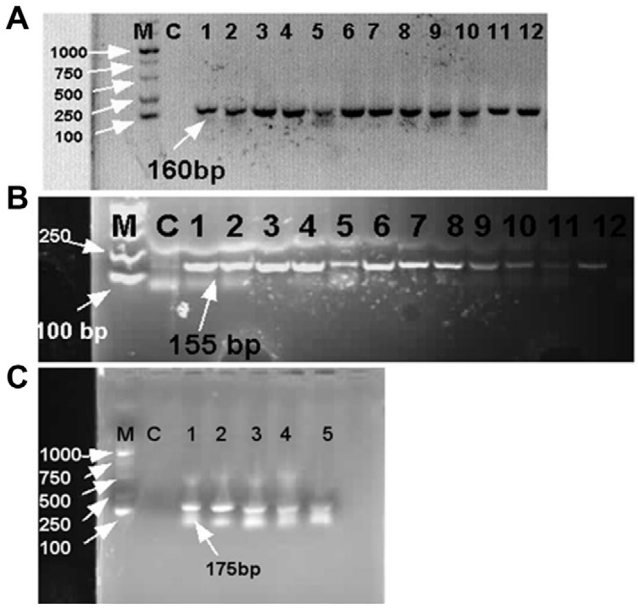

Fig. 4. Polymerase chain reaction (PCR) identification of *Xanthomonas euvesicatoria* on *Physalis pubescens*. (A) The identification *X. euvesicatoria* through *hrpB1* gene of PCR product in which lane M showed DNA molecular weight marker ladder from 100 to 1,000 bp, lane C show control treatment or healthy DNA sample and lanes 1 to 12 expressed disease samples that collected from field and showed amplification with 160 bp amplicon size on 1% agarose gel electrophoresis. (B) Identification of PCR products through *hrpB2* gene. Lane 1 to 12 disease samples showed amplification with 155 bp amplicon size on 1% agarose gel electrophoresis. (C) PCR analysis of five disease samples with specific target gene "*recQ*" and PCR products showed amplification with 175 bp amplicon size on 1% agarose gel electrophoresis.

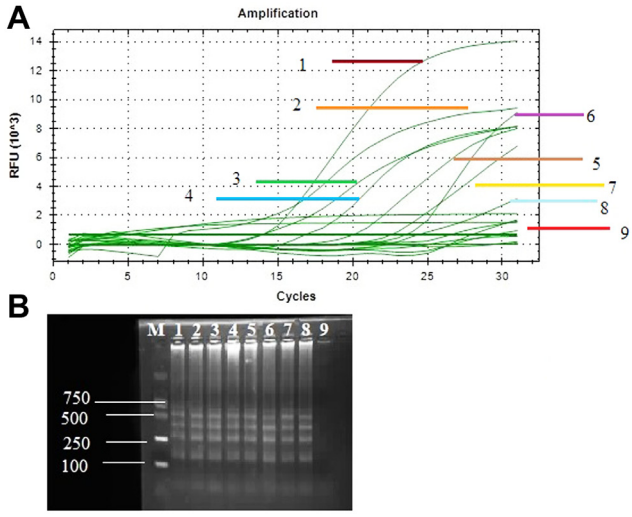

Fig. 5. Sensitive detection of *Xanthomonas euvesicatoria* through loop-mediated isothermal amplification (LAMP) and quantitative polymerase chain reaction assay with primers of specific target gene RecQ. (A) Sensitivity tests performed using CFU BioRed positive results signified with a sigmoid curve. Samples (1-9) used for detection of *X. euvesicatoria*, among these samples 1-8 samples showed positive results and sample 9 was non-template control and showed negative result. (B) Agarose gel electrophoresis of LAMP product on 1.5% agarose gel. M, DNA marker; lanes 1-8, diseased samples; lane 9, non-template control.

LAMP reaction for *X. euvesicatoria* were found at 1.6 µM for internal primers (FIP and BIP) followed by 0.2 µM of outer primers (F3 and B3) with ratio (1:8) and 0.8 µM for loop primers (LF and LB), 1.4 mM for dNTPs, 8 mM for $MgSO_4$, 1× isothermal amplification buffer, 1 U of Bst2.0 WarmStart DNA polymerase (Supplementary Fig. 2A-E). Optimum temperatures of 61°C, 63°C, and 65°C were observed and showed clear band on agarose gel (Supplementary Fig. 2B). The best temperature and time were found at 63°C for 45 min, and final melting temperature was conducted at 83°C for 10 min, and at the end of reaction 125 µM of HNB was used for color visualization. All positive samples of LAMP products were visualized amplification look like ladder-shaped bands and additionally, HNB dye analysis indicated that color change from violet to sky blue for positive amplification, whereas negative samples showed no change in color (Supplementary Fig. 2G). On a 2% agarose gel blemished with one-liter ethidium bromide, the reaction yields were examined; ladder-shaped bands confirmed the efficacy of the LAMP primers.

LAMP assay for sensitivity. The LAMP reaction utilized template target DNA collected from diseased samples using the extraction procedures mentioned above. The sensitivity of the LAMP was measured by 10-fold serial dilution of infected DNA of *P. pubescens*. The sensitivity of the LAMP test ranged from 1×10^{-1} ng/µl to 1×10^{-5} ng/µl when observed with the naked eye. To confirm the amplification, the LAMP reaction products were run through a 2 percent agarose gel electrophoresis (Supplementary Fig. 2F). Sensitivity of template DNA for LAMP reaction ranged from 1×10^{-1} ng/µl to 1×10^{-4} ng/µl was observed but the amplification of 1×10^{-5} ng/µl was not clearly shown on agarose gel electrophoresis.

LAMP and real-time PCR based assay for detection of infected field samples. The disease samples were collected from different parts of the region of Heilongjiang Province, China. The performance of the LAMP assay and real-time PCR with specific target gene *recQ*, used for rapid and

sensitive identification of all diseased samples. Positive amplification showed different ladder-shaped bands on 2% agarose gel electrophoresis while the negative sample showed no band on agarose gel electrophoresis. Therefore, infected samples showed positive amplification with amplified genes and no amplification product was obtained from NTC (Fig. 5B). Real-time PCR assay was also performed for sensitivity analysis of diseased samples. Amplification curves were observed for *recQ* genes in diseased and healthy samples. Positive amplification showed top curves from the bottom and reach their plateau between 7 relative fluorescence units (RFU) 10^3 to 14 RFU10^3 and negative amplification observed curve at the bottom of plot with zero RFU10^3 value (Fig. 5A).

Phylogenetic tree analysis and model design. Phylogenetic analysis is important for analyzing developmental events that occur during evolution, as well as gaining information on biological diversity and genetic classifications. It also depicts the evolutionary history or affiliation between different species, individuals, or organism characters that have adapted from a common ancestor.

In this study, sequence of *hrpB1*, *hrpB2*, and *recQ* genes were used for constructed the phylogenetic tree, and all the phylogenetic trees were conducted in MEGA 11 and furthermore, for well explained the phylogenetic trees designed by itol (https://itol.embl.de/). Model assortment is deliberated as an important phase in the process of building an evolutionary tree. We performed phylogeny inference under common models of DNA sequence evolution. Major 24 fit models of nucleotide substitutions designed in which assessed different models, i.e., T92, K2, HKY, TN93, JC, and GTR joined using the proportion of invariable sites (+I), rate heterogeneity across sites (+G), or both (+I+G) (Supplementary Table 1). Results showed that Tamura 3-parameter (T92) model was best the model for building evolutionary tree through ML method of nucleotide substitution. The Bayesian information criterion (BIC) (Schwarz, 1978) and corrected Akaike information criterion (Hurvich and Tsai, 1989) criterion were used to determine the goodness-of-fit of each model to the data. Tamura 3-parameter (T92) model was obtained the lowermost BIC scores as compared to another modal in Supplementary Table 1. Thus, in this study Tamura 3-parameter (T92) model was used as for more accurate evolution of building evolutionary tree by ML method.

Phylogenetic tree analysis with *recQ*, *hrpB1*, and *hrpB2* genes. In this study, the evolutionary history of the sequences of *recQ*, *hrpB1*, and *hrpB2* were inferred by using

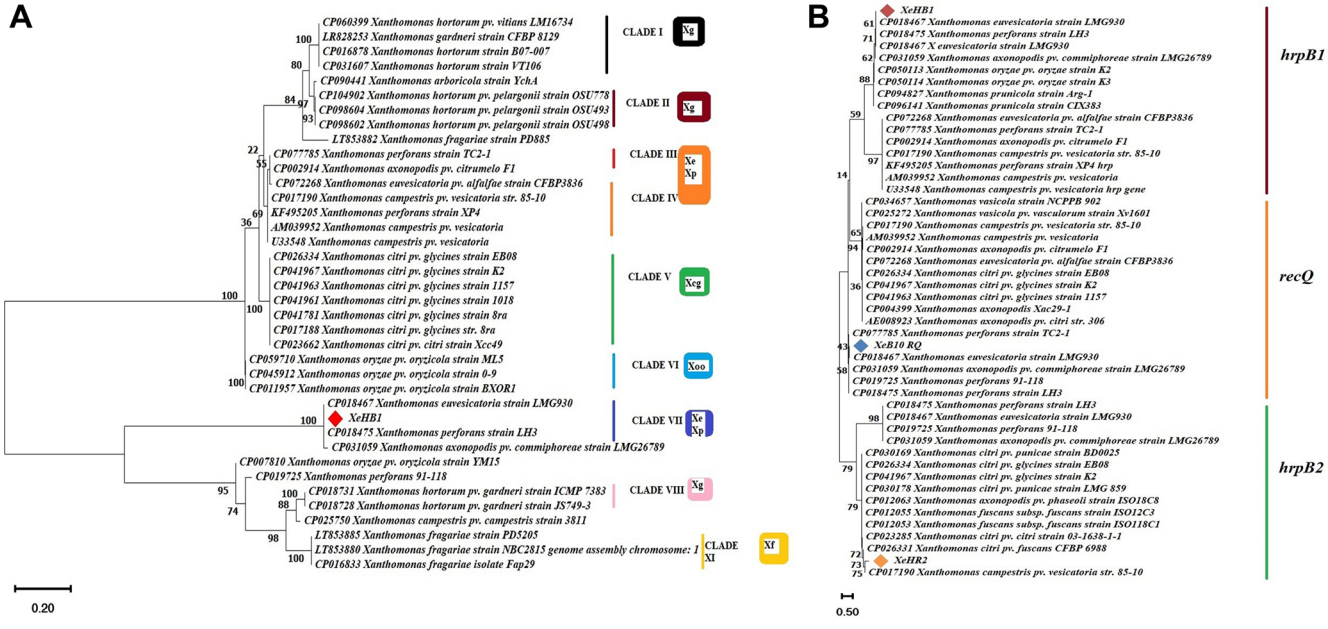

Fig. 6. Phylogenetic tree analysis of *Xanthomonas euvesicatoria* by means of type III secretion system genes "*hrpB1 and hrpB2*" and *recQ* with other *Xanthomonas* strains. Phylogenetic tree was performed through maximum likelihood method that was conducted in MAGA 11. (A) Individual phylogenetic tree analysis using *hrpB1* gene, phylogram from Clade I-Clade IX, *Xanthomonas* strain XeHB1 was closely relative to strains *X. euvesicatoria* LMG930 that have accession no. CP018467 at Clade VII. (B) Combined phylogenetic tree analysis using *hrpB1*, *hrpB2*, and *recQ* genes sequences obtained from polymerase chain reaction products.

more prominent evolutionary history method the Neighbor-Joining method with bootstrap 1,000 replicates (Saitou and Nei, 1987). The evolutionary distances were computed using the Maximum Composite Likelihood method (Tamura et al., 2004). This analysis involved 48 nucleotide sequences. All ambiguous positions were removed for each sequence pair. There were a total of 759 positions in the final dataset. Evolutionary analyses were conducted in MEGA11 (Tamura et al., 2021). Sequences of different organisms used in this study were retrieved from NCBI database and all sequences were aligned through ClustalW. Evolutionary results showed that the sequence of strain XeHB1 was tightly clustered and homology corresponding with strain *X. euvesicatoria* LMG930 and in contrast, no strains were found to *X. vesicatoria* and *X. gardneri* (Fig. 6B). Furthermore, single gene phylogenetic tree analysis using *hrpB1* gene was also performed for more accurate analysis. It was determined that the ML approach and the Tamura 3-parameter (T92) model were the best tools for deducing the evolutionary history (Tamura, 1992). Initial tree(s) for the heuristic search were obtained automatically by applying the Neighbor-Join and BioNJ algorithms to a matrix of pairwise distances estimated using the Tamura 3-parameter (T92) model, and then selecting the topology with the superior log likelihood value. The tree has been drawn to scale, and the length of each branch is indicated by the number of substitutions that have occurred at each site. In this particular investigation, there were 38 nucleotide sequences involved. The completed dataset contained 520 positions in total across its entirety. These results reveal that strain XeHB1 was 99-100% homology corresponding with strain *X. euvesicatoria* LMG930 and *X. perforans* LH3 (Fig. 6A). On the other hand, strain XeHR2 was closely relative to *X. campestris* pv. *vesicatoria* (strain 85-10) (Fig. 6B). Therefore, evolutionary tree analysis with *hrpB1* and *hrpB2* genes showed that all the reference strains were closely relative to *X. euvesicatoria*, *X. campestris* pv. *vesicatoria* (strain 85-10) and did not find *X. vesicatoria* and *X. gardneri*. The results of a whole genome comparison between *X. euvesicatoria* LMG930 and *X. campestris* pv. *vesicatoria* (strain 85-10) revealed that the sequences of both genomes were closely related, with an ANI of 99.94% (Fig. 2). The evolution of the *recQ* gene demonstrated that the strain XeB10RQ was more compatible with the strain *X. euvesicatoria* LMG930 (Fig. 6B).

Phylogenetic tree analysis with specific target gene *recQ* helicase. Evaluation of strains *X. euvesicatoria* with specific target gene *recQ* was conducted through evolutionary history analysis. Comparative analysis of different sequences from target gene *recQ* were retrieve from NCBI database with specific host, origin and species. Phylogenetic tree analysis was conducted for the evaluation of the four strains XeC10RQ, XeH9RQ, XeA10RQ, and XeB10RQ with other *Xanthomonas* strains. Other species of *Xanthomonas* included *X. citri* pv. *citri*, *X. fuscans* subsp.

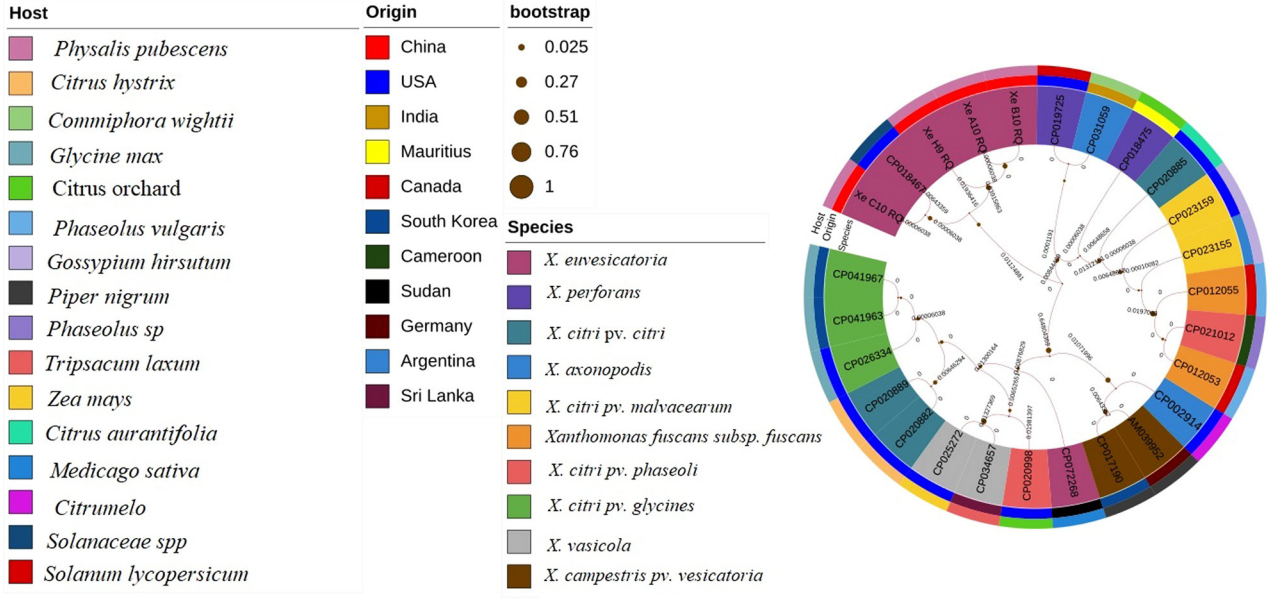

Fig. 7. Phylogenetic tree analysis of *Xanthomonas euvesicatoria* strains (Xe C10 RQ, Xe H9 RQ, Xe A10 RQ, and Xe B10 RQ) through ATP-dependent DNA helicase gene "recQ" performed using maximium likelihood method with host, origin, and species.

fuscans, *X. axonopodis* pv. *citrumelo*, *X. vasicola*, *X. vasicola* pv. *vasculorum*, and *X. citri* pv. *glycines* that cause different diseases such as citrus canker, common bacterial blight, citrus bacterial spot, *Xanthomonas* wilt, bacterial leaf streak, and bacterial pustules, respectively. Phylogenetic tree analysis was inferred by most common method the ML method with 1,000 bootstraps replicates. Results showed that *X. euvesicatoria* strains XeC10RQ, XeH9RQ, XeA10RQ, and XeB10RQ which originated from China on the host *P. pubescens* were closely relative and homology with the strain *X. euvesicatoria* LMG 930 (accession no. CP018467) which origin from USA on *Piper nigrum* (Fig. 7). Evolutionary history showed that these four strains were no found homology with *X. perforans*, *X. axonopodis*, *X. vesicatoria*, and *X. gardneri* that cause BLS disease.

Furthermore, color-coded matrix analysis was designed for pairwise identical sequences. Color-coded matrix results showed that the sequence of the strain XeC10RQ was found 100% homology and identical of the sequence with the strain *X. euvesicatoria* LMG 930 (CP018467) in contrast other three strains showed 95% to 98% homology with the strain *X. euvesicatoria* LMG 930 (CP018467) (Fig. 8). All *Xanthomonas* strains details with accession number, host, origin disease and reference existed in Supplementary Table 2.

Pathogenicity, confirmation, and disease severity analysis of *X. euvesicatoria* using *hrpB1*, *hrpB2*, and *recQ*. All inoculated leaves of *P. pubescens* showed *Xanthomonas* signs of bacterial spot. Symptoms were observed after 3, 7, 14, and 21 days of post-inoculation. Infection was characterized by water-soaked lesion, rupture leaf lamina, necrotic lesion with a yellow margin, necrosis with chlorosis margin, and deformation of leaf but in some leaves showed a black spot on lesion, and after that turn to black color with greasy appearance, whereas bacterial population grows on nutrient agar showed yellow colonies and healthy leaves used as negative control (Supplementary Fig. 3).

Disease severity was observed on five cultivars of *P. pubescens* and measured by Canopeo app (Patrignani

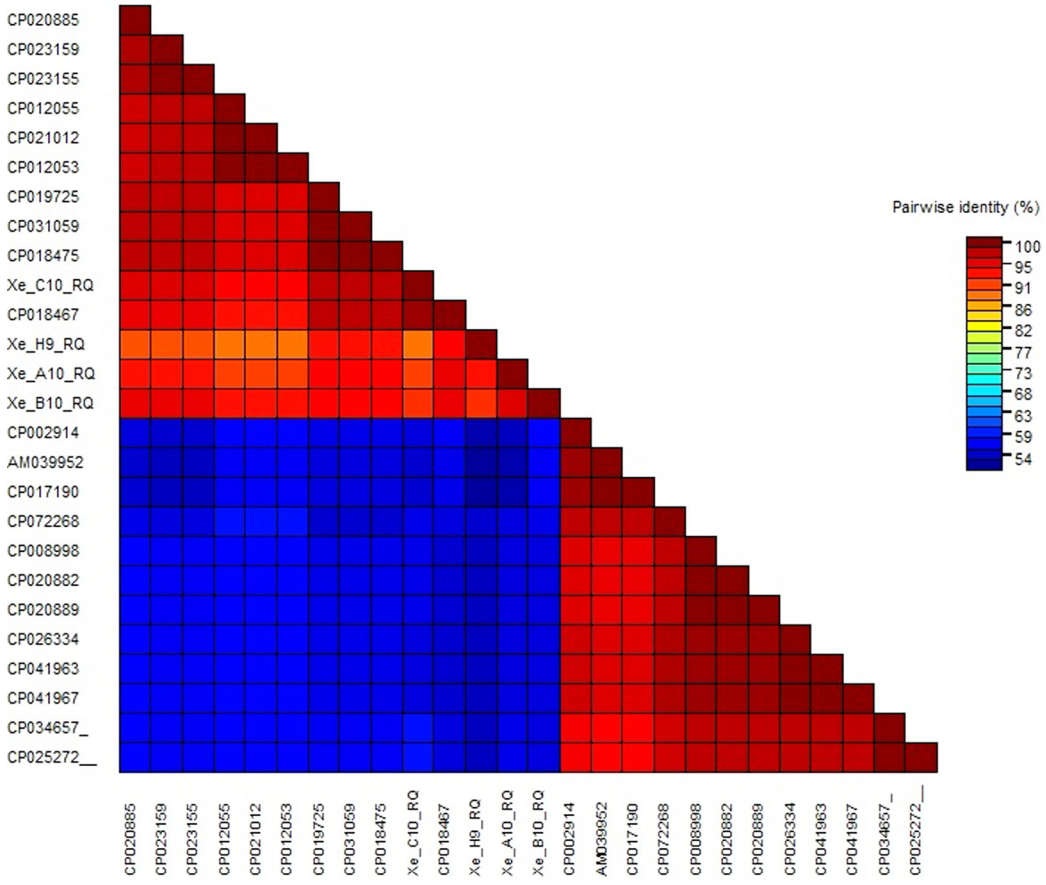

Fig. 8. Color-coded matrix viewing pairwise similarity of *Xanthomonas euvesicatoria* strains (Xe C10 RQ, Xe H9 RQ, Xe A10 RQ, and Xe B10 RQ) with strains of other species. All accession number details used in this study are presented in Supplementary Table 2.

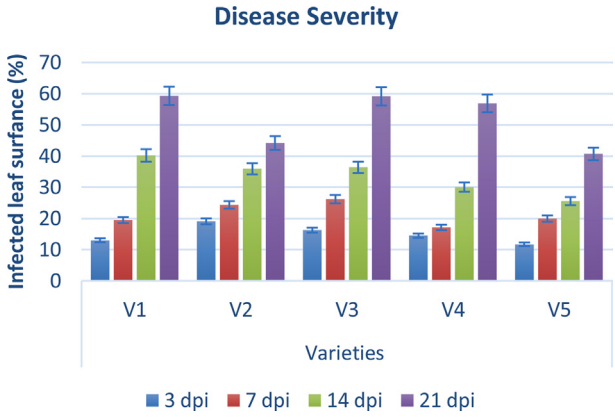

Fig. 9. Bar graph showing disease severity during pathogenicity test assay. y-axis depicted infected leaf area in percentage after inoculation of pathogen and disease symptoms observed at 3, 7, 14, and 21 days of post-inoculation on five varieties (x-axis).

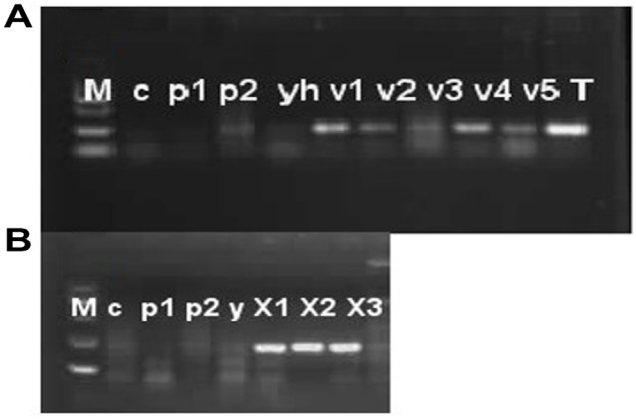

Fig. 10. Pathogenicity test and confirmation assay through polymerase chain reaction on agarose gel electrophoresis with RecQ gene. (A) Specificity and pathogenicity analysis with *recQ* gene primer. Lane M, DNA marker; lane c, healthy leaf; lane p1, *Pseudomonas syringae* pv. *syringae* strain 1; lane p2, *Pseudomonas syringae* pv. *syringae* strain 2; lane yh, *Xanthomonas oryzae* pv. *oryzae*; lane v1, pathogenicity test analysis of variety 1 after inoculation of pathogen; lane v2, pathogenicity test analysis of variety 2 after inoculation of pathogen; lane v3, pathogenicity test analysis of variety 3 after inoculation of pathogen; lane v4, pathogenicity test analysis of variety 4 after inoculation of pathogen; lane v5, pathogenicity test analysis of variety 5 after inoculation of pathogen; lane T, artificial inoculation of pathogen on tomato variety. (B) Confirmation of *X. euvesicatoria* with *recQ* gene. Three *X. euvesicatoria* strains Xeu1, Xeu2, and Xeu3 were collect from Song et al. (2019) that showed on (B) with X1, X2, and X3, respectively. Lane M, DNA marker; lane c, healthy leaf; lane p1, *Pseudomonas syringae* pv. *syringae* strain 1; lane p2, *Pseudomonas syringae* pv. *syringae* strain 2; lane yh, *Xanthomonas oryzae* pv. *oryzae.*

and Ochsner, 2015) after 3, 7, 14, and 21 days of post-inoculation. Bar graph results showed that disease severity is separated into three types' low severity, intermediate severity, and high severity. Three and 7 days post inoculation existed into low severity and 14 days post inoculation was occurrence in medium severity, while 21 days post inoculation showed high severity (Fig. 9). Low severity was observed between percentage ranges from 13% to 25%, while high severity was observed from 40% to 59% of infected damage surface after inoculation (Fig. 9). PCR analysis was performed for confirmation of *X. euvesicatoria* and specificity of *hrpB1*, *hrpB2*, and *recQ* gene primers. Fifty-two bacterial strains (Supplementary Table 3) were used for the evaluation of tested primers specificity and PCR results showed positive amplification through *recQ*, *hrpB1* and *hrpB2* genes (Supplementary Fig. 4). Furthermore, type bacterial strains of *X. euvesicatoria*, *X. vesicatoria*, *X. gardneri*, and *X. perforans* were obtained from Northeast Agricultural University, Harbin, China. Inoculated samples (v1, v2, v3, v4, v5, and T) were used as reference strains while other bacterial strains (*P. syringae* pv. *syringae* and *X. oryzae* pv. *oryzae*) used for specificity of primers and healthy leaves for negative control. Inoculated samples (v1, v2, v3, v4, v5, and T) indicated positive amplification, whereas two strains of *P. syringae* pv. *syringae* (Pss1 and Pss2), *X. oryzae* pv. *oryzae* strain (YH) and healthy leaf (c) showed negative amplification on 1% agarose gel electrophoresis (Fig. 10A). Furthermore, PCR analysis was conducted for confirmation of *X. euvesicatoria* with *hrpB1*, *hrpB2*, and *recQ* genes by using strains Xeu1, Xeu2, and Xeu3 that were collected from Song et al. (2019) (Fig. 10B).

Discussion

P. pubescens is mostly grown in Heilongjiang Province, China's northeast and there are numerous additional informal Chinese names, such as "gu niao" and "mao suan jiang." Its fruit is a sphere-shaped berry that ripens from green to yellow and has a diameter of 1.25 to 2.50 cm. It is fully coated with a flimsy tenacious calyx through its development and ripening. (Luchese et al., 2015). BLS is a worldwide problem caused by four *Xanthomonas* species such as *X. euvesicatoria*, *X. gardneri*, *X. perforans*, and *X. vesicatoria*. Under unfavorable conditions, these four species can cause a 50% yield loss in tomato and pepper plants (Dhakal et al., 2019) but now a day, first identified *X. euvesicatoria* pv. *euvesicatoria* on *P. pubescens* and caused severe economic losses reported by Song et al. (2019). In

our study, 52 pathogenic isolates were obtained from bacterial spot lesions on *P. pubescens* plants throughout Heilongjiang Province, China.

Comparative genome and phylogenetic tree analysis have important factors to illustrate the commonalities and dissimilarities in structure and function (Alzahrani et al., 2021). Next-generation sequencing technologies have established a framework for searching for unique gene sequences, permitting the development of highly specific, trustworthy, and robust field-deployable assays (Ouyang et al., 2013). In our study, we performed a comparative genome analysis of 13 genomes that are closely relative to each other through two more prominent methods Blast comparison and ANI, and data were retrieved from NCBI database facilitating identification and selection of specific target gene "*recQ*". *recQ* helicases are important components of DNA renovation and recombination processes involved in genome integrity (Hartung and Puchta, 2006). Following an evolutionary approach, we explored the DNA repair gene in the genomes of the *Xanthomonadales* group to better understand the methods by which these organisms respond to environmental stressors, such as plant infection. Our comparative genome results showed that the whole genome sequence of *X. euvesicatoria* strain LMG930 was closely relative and 98-99% homology with genome sequence of *X. compestris* pv. *vesicatoria* strain 85-10 *X. perforans* LH3 and *X. axonopodis* pv. *citrumelo* F1 (Figs. 1 and 2). In contrast, *X. euvesicatoria* strain LMG930 found 93%, 89%, 86%, 86%, 85%, 85%, 85%, and 78% homology with *X. citri* pv. *glycines*, *X. vasicola*, *X. hortorum* pv. *gardneri*, *X. arboricola*, *X. fragariea*, *X. vesicatoria*, *X. cucurbitea*, and *X. translucens*, respectively. Therefore, phylogenetic analysis of whole genome sequence through ANI showed clearly that strain *X. euvesicatoria* is very closely relative to strains *X. compestris* pv. *vesicatoria* strain 85-10 *X. perforans* LH3 and *X. axonopodis* pv. *citrumelo* F1 while other strains were found large genetic diversity with *X. euvesicatoria*.

recG, a gene specific to *X. euvesicatoria*, was discovered primarily to the employment of MAUVE to investigate the evolution of *Xanthomonas* species on a large scale (Larrea-Sarmiento et al., 2018). Darling et al. (2010) emphasized that the multiple genome alignments generated by MAUVE progressive for comparative genomic, population genomic studies, and selection and location of genes in the genomes. In our study, using MAUVE multiple alignments to find out location of target gene, we emphasized that the *recQ* gene, which encodes the ATP-dependent DNA helicase, was found in the genomes of *X. euvesicatoria*, *X. axonopodis* pv. *citrumelo* F1, *X. gardneri*, *X. perforans*, and *X. campestris* pv. *vesicatoria* at the position of 3,516,837-3,518,633 bp in all genomes.

In previous studies, molecular diagnosis's potential for *X. euvesicatoria* through multiplex PCR, nested-PCR, real-time PCR (qPCR), conventional PCR, LAMP-PCR, droplet digital PCR, fluorescence *in situ* hybridization, and Box element PCR (BOX-PCR) have been described (Kositcharoenkul et al., 2011; Munhoz et al., 2011). PCR based techniques have been used for pathogen recognition for more than 30 years and are one of the numerous DNA-based fast approaches. In contrast, different researchers (Larrea-Sarmiento et al., 2018; Strayer et al., 2016; Yasuhara-Bell et al., 2017) focus on LAMP technology as compared to PCR. However, we compared conventional PCR, LAMP, and RT-PCR were used for rapid, accurate, and more sensitive identification of *X. euvesicatoria* on *P. pubescens.* Concluded that among molecular approaches LAMP was less timely and costly for pathogen diagnosis detection rather than PCR and qPCR analysis. Molecular evolution of X. *euvesicatoria* on *P. pubescens* through conventional PCR with selected genes *hrpB1* and *hrpB2* type III-secreted proteins that are mostly critical for pathogenicity and detection of *Xanthomonas* pathogens. According to Teper et al. (2016), a T3SS pathway transports effector proteins into host cells to overcome plant resistance and encourage disease influences *X. euvesicatoria* pathogenicity.

Our PCR results showed that all the infected samples were found positive amplification with 160 bp and 155 bp, respectively on agarose gel electrophoresis (Fig. 4). In contrast, we also developed validated and a colorimetric-based LAMP approach for detecting *X. euvesicatoria* on *P. pubescens* that is specific, sensitive, reliable, and resilient. LAMP optimization analysis revealed that concentrations of primer, Bst and $MgSO_4$ were found at 1:8, 1, and 8 mM, respectively on the 61°C at 45 min. Moreover, in our study, betaine concentrations (0.4, 0.6, 0.8, 1, 1.2, and 1.4 M) did not find significantly affected by chemicals reaction. Positive results showed clearly like as different ladder band on agarose gel electrophoresis.

Furthermore, for more accurate results colorimeter analysis developed through HNB and positive amplifications were found the color change from dark blue to violet sky and negative samples showed no change in color. BLS four infections generated considerable economic losses, according to Larrea-Sarmiento et al. (2018) and they also compared the genomes of *X. gardneri*, *X. vesicatoria*, *X. euvesicatoria*, and *X. perforans* to those of other *Xanthomonas* species, and the gene recG was utilized to construct primers for a LAMP assay for fast and effective identification. We compared all molecular approaches for investigation

and quick detection of *X. euvesicatoria* and concluded that LAMP has a novel technique for addressing the shortcomings of PCR-based technologies (Niessen, 2015). The most widely used isothermal-based detection technology is LAMP due to its rapidity, ease of use, increased sensitivity, and compatibility with a variety of detection chemicals. Most importantly, it is simple to do at the point of care as compared to PCR-based detection methods.

The sensitivity of the fabrication LAMP test was verified to ratify the finding bounds in the presence and absence of tested DNA. Sensitivity of LAMP fluctuates by the pathogen, according to Schrader et al. (2012), possibly related to bacterial functional features such as extracellular polysaccharide-producing vs. non-producing bacteria. We observed the sensitivity of the LAMP was tested using a 10-fold serial dilution of *P. pubescens* infected DNA ranging from 1×10^{-1} to 10^{-5} ng/μl. The sensitivity of template DNA for the LAMP reaction ranged from 1×10^{-1} to 10^{-4} ng/μl because amplification of 1×10^{-5} ng/μl on gel electrophoresis was not clearly visible.

Among evolutionary methods, phylogenetic tree is more reliable to find out evolutionary history and detection of *X. euvesicatoria* with specific target or housekeeping genes (Song et al., 2019). Many researchers have studied the detection of *X. euvesicatoria* through the phylogenetic trees on tomato and pepper plants (Kyeon et al., 2016; Roach et al., 2018; Yaripour et al., 2017). In this study, phylogenetic tree analysis was performed with T3SS genes (hrpB1 and hrpB2) with 1000 bootstraps through ML method and found that strains XeHB1 and XeHR2 were closely relative to *X. euvesicatoria* strains (LMG930), *X. perforans* strains (LH3), and *X. campestris* pv. *vesicatoria* (strain 85-10) and this indicates that all tested strains existed in *X. euvesicatoria* because ANI and blast comparison results indicated that the genome of *X. euvesicatoria* showed 99.94% and 98% ANI with *X. perforans* and *X. campestris* pv. *vesicatoria* (strain 85-10) respectively whereas, no tested strains were found homology with *X. vesicatoria* and *X. gardneri.* A circular phylogenetic tree using *recQ* gene showed that four strains XeC10RQ, XeH9RQ, XeA10RQ, and XeB10RQ isolated from *P. pubescens* that collected in Heilongjiang Province, China were very closely relative and maximum homology with strain *X. euvesicatoria* LMG930 from USA on *Piper nigrum*. Furthermore, color-coded pairwise identity matrix showed that XeC10RQ, XeH9RQ, XeA10RQ, and XeB10RQ found 95-99% pairwise identity with strain *X. euvesicatoria* because *recQ* has the ability to DNA repair and recombination pathways elaborate in the looking after of genome reliability (Hartung and Puchta, 2006).

Pathogenicity studies revealed that *X. euvesicatoria* was found on all inoculated *P. pubescens* as well as tomato plants (Jones et al., 2004). Following 3, 7, 14, and 21 days after inoculation, symptoms were detected (Supplemenary Fig. 3). The Canopeo app measured disease severity 3, 7, 14, and 21 days after inoculation (Patrignani and Ochsner, 2015). The severity of the disease was categorized into three types: low, intermediate, and high. After inoculation, low severity was observed between percentage ranges of 13% to 25%, whereas high severity was reported between 40% and 59% of infected damage surface (Fig. 9). According to Hernández-Huerta et al. (2021), *Xanthomonads* were grouped into three groups in a cluster analysis of bacterial spot severity according to their virulence and findings that isolated *X. euvesicatoria* caused medium damage 76.8% final severity and low damage 29.8% final severity.

Conflicts of Interest

No potential conflict of interest relevant to this article was reported.

Acknowledgments

We are especially thankful to Dr. Shuang Song (Assistance Professor, Northeast Agricultural University) for providing *Xanthomonas euvesicatoria* inoculum (Xeu1, Xeu2, and Xeu3). This research was funded by “Precision poverty alleviation project of planting industry science and technology, special project of central leading local science and technology development, grant number ZY18C08”, “Isolation and identification of candidate genes related to response to the stress of Magnaporthe grisea in rice, nature fund project, Heilongjiang, China, grant number C2017032”, and “Integration and extension of green control techniques for rice diseases in main rice production areas of Heilongjiang, grant number GA19B104”.

Electronic Supplementary Material

Supplementary materials are available at The Plant Pathology Journal website (http://www.ppjonline.org/).

References

Alzahrani, D., Albokhari, E., Yaradua, S. and Abba, A. 2021. Complete chloroplast genome sequences of *Dipterygium glaucum* and *Cleome chrysantha* and other *Cleomaceae* species, comparative analysis and phylogenetic relationships. *Saudi J. Biol. Sci*. 28:2476-2490.

Baker, R., Bragard, C., Candresse, T. Gilioli, G., Grégoire, J.-C., Holb, I., Jeger, M. J., Karadjova, O. E., Magnusson, C., Makowski, D., Manceau, C., Navajas, M., Rafoss, T., Rossi, V., Schans, J., Schrader, G., Urek, G., van Lenteren, J. C., Vloutoglou, I., Winter, S. and van der Werf, W. 2014. Scientific opinion on the pest categorisation of *Xanthomonas campestris* pv. *vesicatoria* (Doidge) dye. *EFSA J.* 12:3720.

Ciria, R., Abreu-Goodger, C., Korett, E. and Merino, E. 2004. GeConT: gene context analysis. *Bioinformatics* 20:2307-2308.

Darling, A. E., Mau, B. and Perna, N. T. 2010. progressiveMauve: multiple genome alignment with gene gain, loss and rearrangement. *PLoS ONE* 5:e11147.

Dhakal, U., Dobhal, S., Alvarez, A. M. and Arif, M. 2019. Phylogenetic analyses of xanthomonads causing bacterial leaf spot of tomato and pepper: *Xanthomonas euvesicatoria* revealed homologous populations despite distant geographical distribution. *Microorganisms* 7:462.

EFSA Panel on Plat Health (PLH). 2014. Scientific opinion on the pest categorization of *Xanthomonas campestris pv. vesicatoria* (Doidge) dye. *EFSA J.* 12:3720.

El Sheikha, A. F. 2004. Technological, chemical and microbiological studies on some packed foods. M.S. thesis. Faculty of Agriculture, Minufiya University, El-Kom, Egypt. 174 pp.

El Sheikha, A. F., Piombo, G., Goli, T. and Montet, D. 2010. Main composition of Physalis (*Physalis pubescens* L.) fruit juice from Egypt. *Fruits* 65:255-265.

Garita-Cambronero, J., Palacio-Bielsa, A. and Cubero, J. 2018. *Xanthomonas arboricola* pv. *pruni*, causal agent of bacterial spot of stone fruits and almond: its genomic and phenotypic characteristics in the *X. arboricola* species context. *Mol. Plant Pathol*. 19:2053-2065.

Hao, X.-L., Zhang, J.-J., Li, X.-H. and Wang, W. 2017. Application of a chitosan coating as a carrier for natamycin to maintain the storage quality of ground cherry (*Physalis pubescens* L.). *J. Zhejiang Univ. Sci. B* 18:807-815.

Hartung, F. and Puchta, H. 2006. The RecQ gene family in plants. *J. Plant Physiol.* 163:287-296.

Hernández-Huerta, J., Tamez-Guerra, P., Gomez-Flores, R., Delgado-Gardea, M. C. E., García-Madrid, M. S., Robles-Hernández, L. and Infante-Ramirez, R. 2021. Prevalence of *Xanthomonas euvesicatoria* (formally *X. perforans*) associated with bacterial spot severity in *Capsicum annuum* crops in south central Chihuahua, Mexico. *PeerJ* 9:e10913.

Hurvich, C. M. and Tsai, C.-L. 1989. Regression and time series model selection in small samples. *Biometrika* 76:297-307.

Jones, J. B., Lacy, G. H., Bouzar, H., Stall, R. E. and Schaad, N. W. 2004. Reclassification of the xanthomonads associated with bacterial spot disease of tomato and pepper. *Syst. Appl. Microbiol.* 27:755-762.

Kebede, M., Timilsina, S., Ayalew, A., Admassu, B., Potnis, N., Minsavage, G. V., Goss, E. M., Hong, J. C., Strayer, A., Paret, M., Jones, J. B. and Vallad, G. E. 2014. Molecular characterization of *Xanthomonas* strains responsible for bacterial spot of tomato in Ethiopia. *Eur. J. Plant Pathol*. 140:677-688.

Kositcharoenkul, N., Chatchawankanphanich, O., Bhunchoth, A. and Kositratana, W. 2011. Detection of *Xanthomonas citri* subsp. *citri* from field samples using single-tube nested PCR. *Plant Pathol.* 60:436-442.

Kyeon, M.-S., Son, S.-H., Noh, Y.-H., Kim, Y.-E., Lee, H.-I. and Cha, J.-S. 2016. *Xanthomonas euvesicatoria* causes bacterial spot disease on pepper plant in Korea. *Plant Pathol. J.* 32:431-440.

Larrea-Sarmiento, A., Dhakal, U., Boluk, G., Fatdal, L., Alvarez, A., Strayer-Scherer, A., Paret, M., Jones, J., Jenkins, D. and Arif, M. 2018. Development of a genome-informed loop-mediated isothermal amplification assay for rapid and specific detection of *Xanthomonas euvesicatoria. Sci. Rep.* 8:14298.

Lee, I., Kim, Y. O., Park, S.-C. and Chun, J. 2015. OrthoANI: an improved algorithm and software for calculating average nucleotide identity. *Int. J. Syst. Evol. Microbiol*. 66:1100-1103.

Luchese, C. L., Gurak, P. D. and Marczak, L. D. F. 2015. Osmotic dehydration of physalis (*Physalis peruviana* L.): evaluation of water loss and sucrose incorporation and the quantification of carotenoids. *LWT Food Sci Technol*. 63:1128-1136.

Martins-Pinheiro, M., Galhardo, R. S., Lage, C., Lima-Bessa, K. M., Aires, K. A. and Menck, C. F. M. 2004. Different patterns of evolution for duplicated DNA repair genes in bacteria of the *Xanthomonadales* group. *BMC Evol. Biol.* 4:29.

Mendonca, V. M., Klepin, H. D. and Matson, S. W. 1995. DNA helicases in recombination and repair: construction of a delta uvrD delta helD delta recQ mutant deficient in recombination and repair. *J. Bacteriol.* 177:1326-1335.

Munhoz, C. F., Weiss, B., Hanai, L. R., Zucchi, M. I., Fungaro, M. H. P., Oliveira, A. L. M., Monteiro-Vitorello, C. B. and Vieira, M. L. C. 2011. Genetic diversity and a PCR-based method for *Xanthomonas axonopodis* detection in passion fruit. *Phytopathology* 101:416-424.

Niessen, L. 2015. Current state and future perspectives of loop-mediated isothermal amplification (LAMP)-based diagnosis of filamentous fungi and yeasts. *Appl. Microbiol. Biotechnol.* 99:553-574.

Ouyang, P., Arif, M., Fletcher, J., Melcher, U. and Ochoa Corona, F. M. 2013. Enhanced reliability and accuracy for field deployable bioforensic detection and discrimination of *Xylella fastidiosa* subsp. *pauca*, causal agent of citrus variegated chlorosis using Razor Ex technology and TaqMan quantitative PCR. *PLoS ONE* 8:e81647.

Patrignani, A. and Ochsner, T. E. 2015. Canopeo: a powerful new tool for measuring fractional green canopy cover. *Agron. J.* 107:2312-2320.

Roach, R., Mann, R., Gambley, C. G., Shivas, R. G. and Rodoni, B. 2018. Identification of *Xanthomonas* species associated with bacterial leaf spot of tomato, capsicum and chilli crops in eastern Australia. *Eur. J. Plant Pathol.* 150:595-608.

Saitou, N. and Nei, M. 1987. The neighbor-joining method: a new method for reconstructing phylogenetic trees. *Mol. Biol. Evol*. 4:406-425.

Schrader, C., Schielke, A., Ellerbroek, L. and Johne, R. 2012. PCR inhibitors: occurrence, properties and removal. *J. Appl. Microbiol*. 113:1014-1026.

Schwarz, G. 1978. Estimating the dimension of a model. *Ann. Stat*. 6:461-464.

Song, S., Zhang, Y., Liu, H., Pan, C.-Q., Yang, M.-X., Ding, J.-F. and Zhang, J.-H. 2019. Isolation and characterization of *Xanthomonas euvesicatoria* pv. *euvesicatoria* causing bacterial spot in *Physalis pubescens* in Northeast China. *J. Plant Pathol*. 101:361-366.

Strayer, A. L., Jeyaprakash, A., Minsavage, G. V., Timilsina, S., Vallad, G. E., Jones, J. B. and Paret, M. L. 2016. A multiplex real-time PCR assay differentiates four *Xanthomonas* species associated with bacterial spot of tomato. *Plant Dis.* 100:1660-1668.

Tamura, K. 1992. Estimation of the number of nucleotide substitutions when there are strong transition-transversion and G + C-content biases. *Mol. Biol. Evol*. 9:678-687.

Tamura, K., Nei, M. and Kumar, S. 2004. Prospects for inferring very large phylogenies by using the neighbor-joining method. *Proc. Natl. Acad. Sci. U. S. A.* 101:11030-11035.

Tamura, K., Stecher, G. and Kumar, S. 2021. MEGA 11: Molecular Evolutionary Genetics Analysis version 11. *Mol. Biol. Evol*. 38:3022-3027.

Teper, D., Burstein, D., Salomon, D., Gershovitz, M., Pupko, T. and Sessa, G. 2016. Identification of novel *Xanthomonas euvesicatoria* type III effector proteins by a machine-learning approach. *Mol. Plant Pathol*. 17:398-411.

USDA Natural Resources Conservation Service. 2016. Plants database. *Physalis pubescens*. URL http://plants.usda.gov [31 August 2022].

Yaripour, Z., Mohsen Taghavi, S., Osdaghi, E. and Lamichhane, J. R. 2017. Host range and phylogenetic analysis of *Xanthomonas alfalfae* causing bacterial leaf spot of alfalfa in Iran. *Eur. J. Plant Pathol.* 150:267-274.

Yasuhara-Bell, J., Marrero, G., Arif, M., de Silva, A. and Alvarez, A. M. 2017. Development of a loop-mediated isothermal amplification assay for the detection of *Dickeya* spp. *Phytopathology* 107:1339-1345.

Zhang, Y. and Tanner, N. A. 2017. Isothermal amplification of long, discrete DNA fragments facilitated by single stranded binding protein. *Sci. Rep*. 7:8497.

Zhong, J. and Zhao, X. 2018. Isothermal amplification technologies for the detection of foodborne pathogens. *Food Anal. Methods* 11:1543-1560.